Spectroscopy of ^{18}O: $^{14}C(^{7}Li,t\gamma)^{18}O$ reaction; observation of selective enhanced $E1$ deexcitations of cluster states

M. Gai, M. Ruscev,* and D. A. Bromley†
A. W. Wright Nuclear Structure Laboratory, Yale University, New Haven, Connecticut 06511

J. W. Olness
Department of Physics, Brookhaven National Laboratory, Upton, New York 11973
(Received 29 May 1990)

The alpha-particle transfer reaction $^{14}C(^{7}Li,t\gamma)^{18}O$ was used to study gamma deexcitation modes in ^{18}O at a bombarding energy $E_L=15$ MeV. In this measurement 4×10^6 triton-gamma coincidence events were collected. All natural parity states up to the alpha-particle threshold at 6.227 MeV were studied. These data together with our previously published study of states above threshold, using the $\alpha+^{14}C$ radiative capture reaction, provide relatively complete spectroscopic information on states in ^{18}O up to 8.3 MeV in excitation energy. Previously reported major gamma decay branching ratios were remeasured with higher accuracy and good agreement is found. Several new weak deexcitation modes are reported. Enhanced $E1$ decays, $B(E1)\cong10^{-2}$ Weisskopf unit, were observed among the $J^\pi=0_2^+$, 1_1^-, 1_2^-, 2_3^+, and 3_3^- states, representing some of the most enhanced $E1$'s found in even-even nuclei. A strong empirical correlation between enhanced $E1$ decays and cluster structure is established. These enhanced $B(E1)$'s suggest a selective deexcitation mode in which the states involved preferentially decay to cluster states. The cluster states are strongly populated in cluster transfer reactions and weakly populated in (t,p) reactions. Predictions of the vibron cluster model are compared with our data. The presence in our data of contaminant lines from $^{14}C(^{7}Li,\alpha)^{17}N$ allowed extraction of some information on ^{17}N.

I. INTRODUCTION

The $A=18$ mass chain,[1] and ^{18}O in particular, provides a good illustration of the charge independence of the nucleon-nucleon interaction, and of isospin multiplet structure in light nuclei. In this mass region one finds evidence for coexistence between simple two-neutron shell-model states, multiparticle-multihole collective states, and those apparently having well-defined cluster structure.[2–7] This interplay has prompted extensive experimental[8–19] and theoretical[20–23] effort.

A renewed interest in ^{18}O was generated by the suggestions of Iachello[24] and of Iachello and Jackson[25] that cluster states should yield collective enhanced $E1$ deexcitation transitions. This suggestion is similar to an earlier work of Buck and Pilt,[26] who predicted enhanced $E1$'s linking $t+^{16}O$ cluster states in ^{19}F. In such cluster states, the center of charge is displaced from the center of mass, yielding nuclear polarization and enhanced $E1$ decay matrix elements.[27,28]

Our earlier reports[29,30] on enhanced $E1$ transitions in ^{18}O have resulted in several attempts to reproduce the observed enhancements on the basis of current nuclear-structure models. These included a sum-rule model,[31] a time-dependent Hartree-Fock (TDHF) model,[32] two generator-coordinate-method (GCM) cluster models[33–36] (similar in nature but with contradicting conclusions), and large-basis shell-model calculations.[37,38] While it is clear that cluster states give rise to polarization and thus to enhanced $E1$ deexcitations, it is very difficult to calculate the corresponding matrix elements of cluster states in a microscopic way. The calculations reported to date indicate a sensitive interplay between $E1$ enhancements arising from cluster structure and those arising from complex shell-model admixtures in the state wave functions. On one hand, the sum-rule model of Alhassid, Gai, and Bertsch[31] predicts enhanced $E1$ decays from cluster states with $B(E1)\approx10^{-2}$ Weisskopf unit (W.u.). On the other hand, early estimates of Millener using the Millener-Kurath[21] interaction reveal enhanced $E1$'s arising from two-neutron states which are of the same order of magnitude.

In this paper we report measurements on enhanced $E1$ transitions in ^{18}O and observe that, empirically, the available data exhibit strong selectivity and preferential $E1$ deexcitations to and from cluster collective states. This conclusion is empirical, and therefore *independent of any model prediction.* In Sec. II of this paper we describe the experimental procedures. The experimental results are presented in Sec. III, and in Sec. IV we discuss the nature of the observed enhanced $E1$ transitions. Conclusions are presented in Sec. V.

II. EXPERIMENTAL PROCEDURE

The $^{14}C(^{7}Li,t\gamma)^{18}O$ coincidence experiment was carried out using 15 MeV ^{7}Li beams from the MP1 Yale University tandem. Enriched (96%) self-supporting ^{14}C targets, produced at the Chalk River Laboratories,[39] of areal density 40 $\mu g/cm^2$ were used. The outgoing parti-

cles were detected in a silicon surface-barrier detector in coincidence with gamma radiations detected in a Ge(Li) detector. The particle detector was an annular solid-state detector centered at 0° and placed 3 cm away from the target, subtending a solid angle of 85 msr ($\theta = 10.7° \pm 2.1°$). An aluminum foil, of areal density 42 mg/cm^2, was placed in front of this detector to stop all nuclei heavier than alpha particles. The alpha particles produced in the $^{14}C(^7Li,\alpha)^{17}N$ reaction lose sufficient energy in the foil to be less energetic than tritons corresponding to 6 MeV of excitation energy in ^{18}O. Lighter hydrogen isotopes deposit only a small amount of energy in the detector active volume, permitting accumulation of background-free triton spectra up to energies corresponding to states in $^{18}O \geq 6$ MeV and below. The energy resolution was $\delta E \leq 250$ keV and was primarily limited by straggling in the aluminum foil and by kinematic broadening reflecting the large angular aperture of the detector.

The gamma radiation was detected using a Ge(Li) detector having 20% efficiency relative to a standard 7.5×7.5 cm NaI(Tl) detector. The Ge(Li) detector was placed 3.5 cm away from the target at an angle of 125° with respect to the beam (55° at backward angles), subtending an effective solid angle of 0.68 srad (i.e., $\Delta\theta = 25°$). For the case of dipole and quadrupole radiations the angular distributions can be expressed as

$$W(\theta) = A_0[1 + \alpha_2 Q_2 A_2 P_2(\theta) + \alpha_4 Q_4 A_4 P_4(\theta)] \quad (1)$$

in the usual notation[40,41] where Q_2 is an angular distribution attenuation factor arising from the detector's finite size, and α_4 is a quenching factor arising from the finite m-substate population. For $\theta = 55°$, $P_2 = 0$ and $P_4 = -0.38$ with $Q_4 = 0.5$ for our geometry.[42] With $\alpha_4 = 0.1$,[41] corresponding to detecting the tritons at 10° with a distribution of m substates of $\delta m/J = 0.4$, we estimate the largest contributions from the last term in Eq. (1), for a $2 \rightarrow 0$ transition with $A_4 = -1.71$, to amount to only 3% of the total intensity. For most of the other transitions this contribution is significantly smaller than 1%. By placing our gamma-ray detector at $\theta = 55°$ we were thus able to measure (relative) angle-integrated intensities without measuring complete angular distributions.

The relative efficiency of the gamma detector was measured as a function of energy using ^{152}Eu, ^{228}Th, and ^{56}Co standard sources. The latter was produced via the $^{56}Fe(p,n)^{56}Co$ reaction using proton beams from the Brookhaven National Laboratory cyclotron. These sources allowed calibration of the detector to 3.5 MeV. For higher energies we derived an efficiency curve using published data for a similar detector that defined the expected deviations from an E^{-x} behavior.[43,44] While the large amount of data collected in this work allowed us to measure the deexcitation of states in ^{18}O with excellent statistics, systematic uncertainties in some cases govern the quoted accuracy. In all cases the quoted uncertainties include both statistical and systematic components.

A fast coincidence was required between the particle and gamma ray detectors, with a time resolution of 5 nsec (FWHM). 4×10^6 coincidence events were collected during 85 h with beam on target, with an average beam intensity of 30 charge nA. The average detector counting rates were 3 kHz in the particle detector, and 4.5 kHz in the gamma-ray detector, yielding approximately 16 coincidence events per second.

III. EXPERIMENTAL RESULTS

The natural parity states of ^{18}O populated in the $^{14}C(^7Li,t\gamma)^{18}O$ coincidence experiment are indicated in Fig. 1, which shows the triton spectrum measured in coincidence with gamma radiations having $E_\gamma > 0.511$ MeV. This spectrum appears to be almost free of background for triton groups corresponding to states in ^{18}O below 6 MeV of excitation. All natural parity states up to the alpha-particle threshold, and including the 4_2^+ state at 7.12 MeV, were populated in this reaction. Reflecting the large solid angle of the particle detector, triton groups corresponding to the states of interest are not resolved in this spectrum; however, their respective gamma deexcitations are clearly resolved in the Ge(Li) spectra.

The data reduction was accomplished by gating on different triton groups to establish the coincident gamma spectra. Such spectra thus show the primary gamma deexcitations of the selected states and of the subsequent daughter states in the deexcitation cascade. The branching ratios are then obtained from the relative intensity ratios of the primary transitions, and also from the intensities of the subsequent radiations in the cascade. It was required that the intensities thus obtained be internally consistent. The upper limits obtained in this work were obtained in a similar fashion, and are quoted here at the level of one standard deviation above background (60% confidence level). The gamma spectra are shown in Figs. 2–4. The obtained branching ratios are shown in Fig. 5 and are listed in Table I.

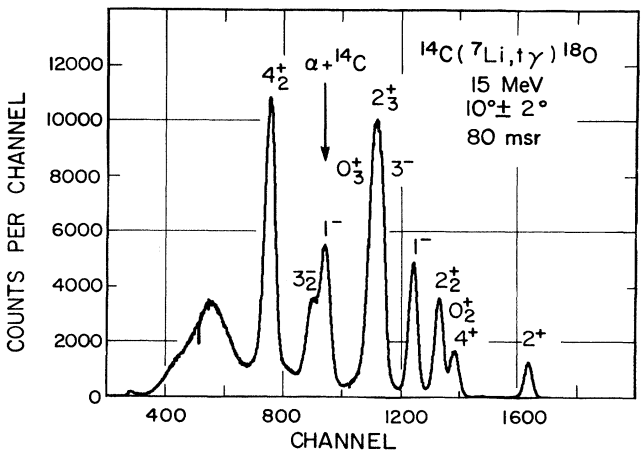

FIG. 1. Triton spectrum measured in coincidence with gamma rays ($E_\gamma > 511$ keV), from $^{14}C(^7Li,t\gamma)^{18}O$. The experimental resolution ($\delta E \leq 250$ keV) reflects the large solid angle of the particle detector and the presence of the aluminum absorber as discussed in the text. The $\alpha + ^{14}C$ threshold is indicated.

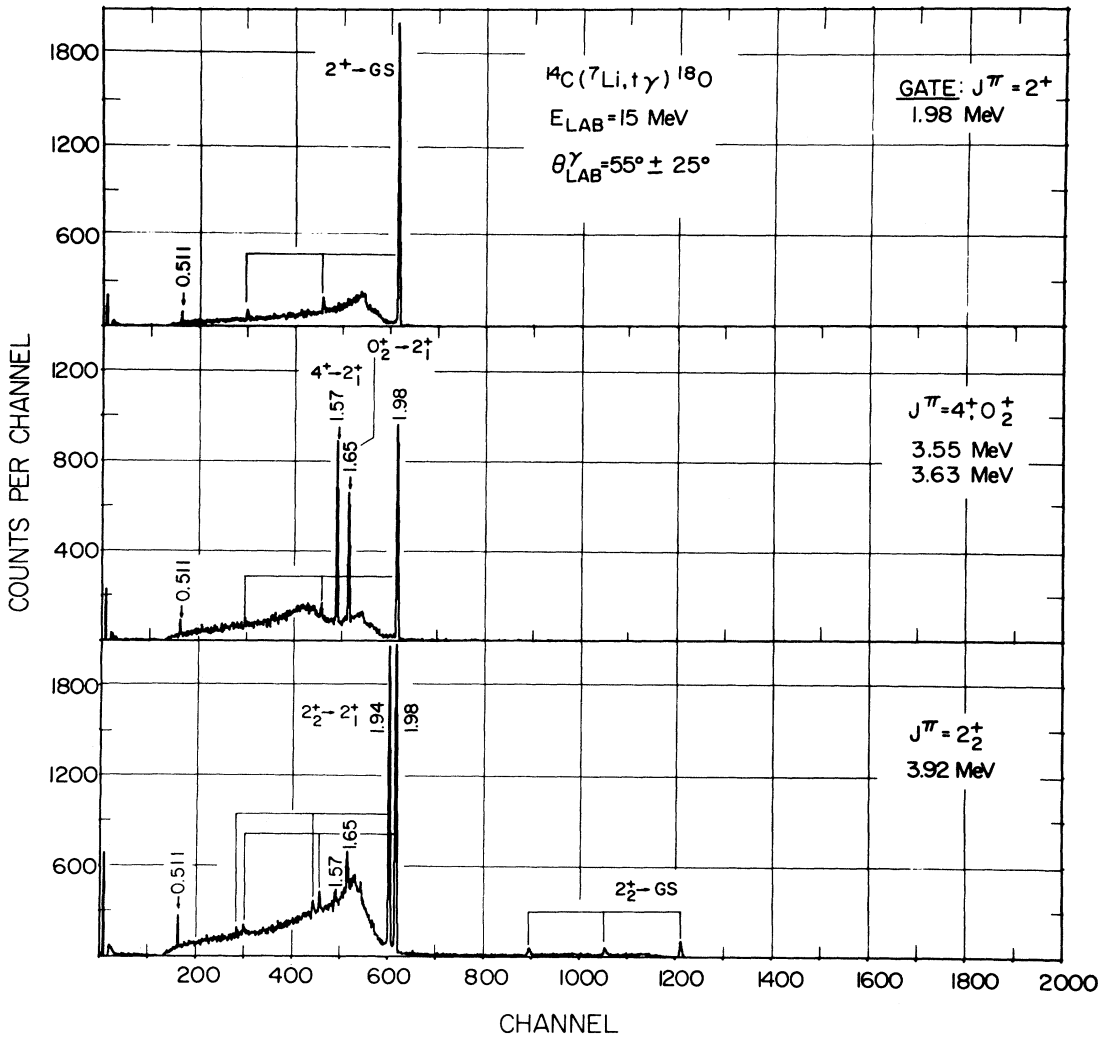

FIG. 2. Gamma-ray spectra in coincidence with specified triton groups.

We note that, for example, the branching ratios in the deexcitation of the 2_2^+ state obtained in this work are $B(2_2^+ \rightarrow 2_1^+)=0.889(10)$ and $B(2_2^+ \rightarrow 0_{g.s.}^+)=0.11(10)$, which are in excellent agreement with those obtained from measurements of complete angular distributions as reported in Ref. 9: i.e., $B(2_2^+ \rightarrow 2_1^+)=0.870(30)$ and $B(2_2^+ \rightarrow 0_{g.s.}^+)=0.130(30)$. We note a small discrepancy between our data and those of Ref. 9 in the case of the deexcitation of the 0_3^+ state for which we quote $B(0_3^+ \rightarrow 1^-)=0.548(50)$ and $B(0_3^+ \rightarrow 2^+)=0.452(50)$, whereas in Ref. 9 we find $B(0_3^+ \rightarrow 1^-)=0.46(5)$, and $B(0_3^+ \rightarrow 2^+)=0.54(5)$. The results, however, are still consistent within the quoted uncertainties.

In addition to the major decay modes in ^{18}O, we also extracted data on very weak branching ratios for the deexcitation of the $J^\pi=2_3^+$ and 3_2^- states and found them to correspond to (unexpectedly) large $B(E2)$ values. Despite the fact that our experimental uncertainties here are large ($\pm 50\%$), we quote these results because of their theoretical importance and as a motivation of future experiments.

The 1.857 MeV deexcitation expected from the $4_2^+ \rightarrow 2_3^+$ transition appears superimposed on the higher-energy tail of the prominent 1.850 MeV deexcitation from ^{17}N; the subsequent deexcitation of the 2_3^+ state ($B=0.559$) was therefore used to extract an upper limit on the intensity of the $4_2^+ \rightarrow 2_3^+$ deexcitation, as listed in Table I. The location of the expected, but not observed line, is also shown in the inset of Fig. 4.

For the extraction of reduced transition rates we used lifetime data quoted in Ref. 1. For the $J^\pi=2_3^+$, 1_2^-, and 4_2^+ states, lifetimes were deduced from (e,e'),[19] (γ,γ'),[11] and alpha particle width data,[45] respectively, together with our measured branching ratios. The reduced matrix elements thus obtained are listed in Table I; the indicated uncertainties include those in the branching ratios and

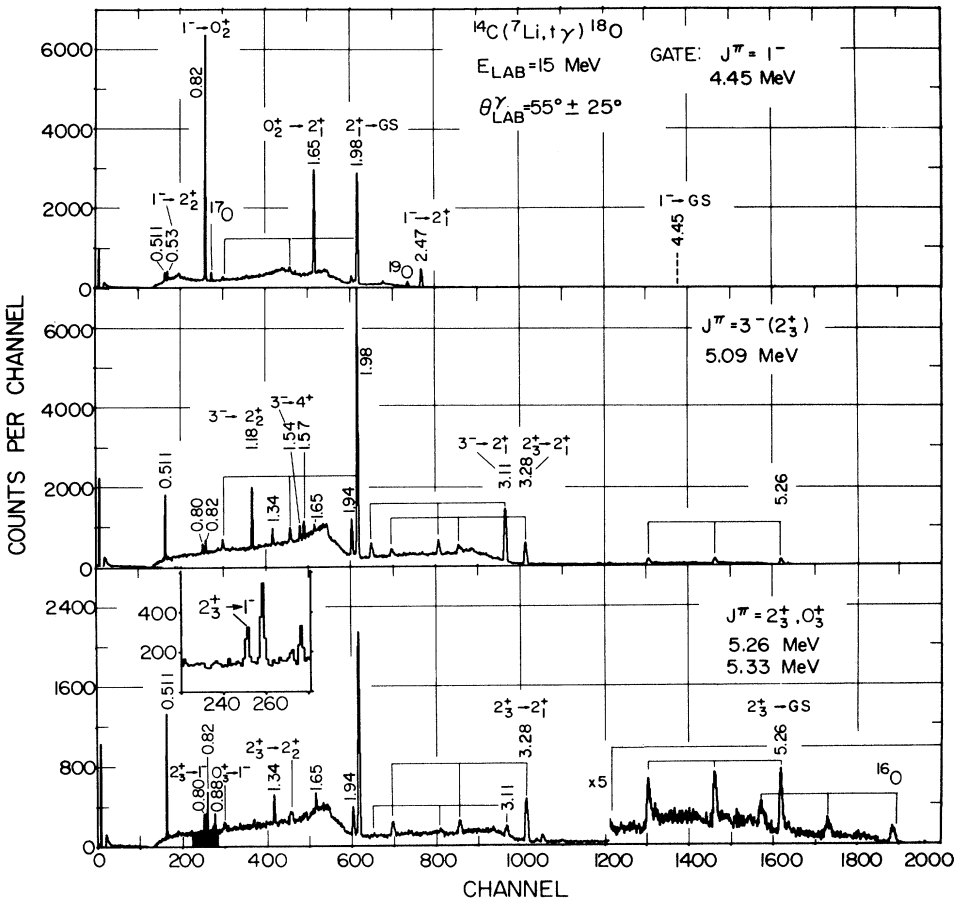

FIG. 3. Gamma-ray spectra in coincidence with specified triton groups. The expected location of the unobserved $1^-_1 \rightarrow 0^+_{g.s.}$ transition is indicated. (Note that in this energy region the background is at a level of 10 counts per channel.) In the inset, we show the enhanced $E1$ deexcitation of the $2^+_3 \rightarrow 1^-$ state.

the lifetimes.

Several contaminant gamma-ray lines originating in ^{19}O, ^{17}O, ^{16}O, and ^{17}N appear in Figs. 3 and 4, from the following reactions: $^{14}C(^7Li,d\gamma)^{19}O$, $^{12}C(^7Li,d\gamma)^{17}O$, $^{12}C(^7Li,t\gamma)^{16}O$, and $^{14}C(^7Li,\alpha\gamma)^{17}N$. These contaminant lines, together with the lines associated with ^{18}O, allow us to account for all gamma-ray lines appearing in our coincidence spectra. We also note the increasing intensity of the annihilation radiation peak at 0.511 MeV—which in the case of the higher states in ^{18}O arises from increased pair production by the higher-energy gamma rays, producing prompt 0.511 MeV radiation at the walls of the scattering chamber. Using the contaminant lines from ^{17}N shown in Fig. 4, we were able to extract major branching ratios for the deexcitation of certain states in ^{17}N, as shown in Fig. 6 and listed in Table II.

IV. DISCUSSION

Below 8.3 MeV excitation in ^{18}O we find three 0^+ states, four 1^- states, four 2^+ states, three 3^- states, and two 4^+ states,[1] for which a major fraction of all possible 46 $E1$ deexcitations have been studied in our previous work[45] and in this work. The corresponding $B(E1)$'s, together with a few additional ones arising from 5^- states and from non-natural parity states, form a substantial statistical sample in which we can search for characteristic trends exhibited by enhanced $E1$ deexcitations in ^{18}O.

In Fig. 7 we show the distribution of the 41 measured $B(E1)$ matrix elements in ^{18}O. All reduced matrix elements smaller then 5×10^{-4} W.u., including some measured upper limits, have been grouped together for presentation here. Larger-value upper limits are not yet sufficiently defined to allow inclusion in our analysis. From the data presented in Fig. 7 we calculate the ensemble average of the $B(E1)$'s in ^{18}O to be 1.6×10^{-3} W.u. with a distribution concentrated between 4.6×10^{-3} and 8.6×10^{-4} W.u. This includes roughly 60% of the data points, as would be the case for a normal distribution. Of particular interest then are the enhanced $E1$'s lying outside this distribution, i.e., seven transitions with $B(E1)\geq0.7\times10^{-2}$ W.u. We first review some of the properties of the states involved in these enhanced $E1$

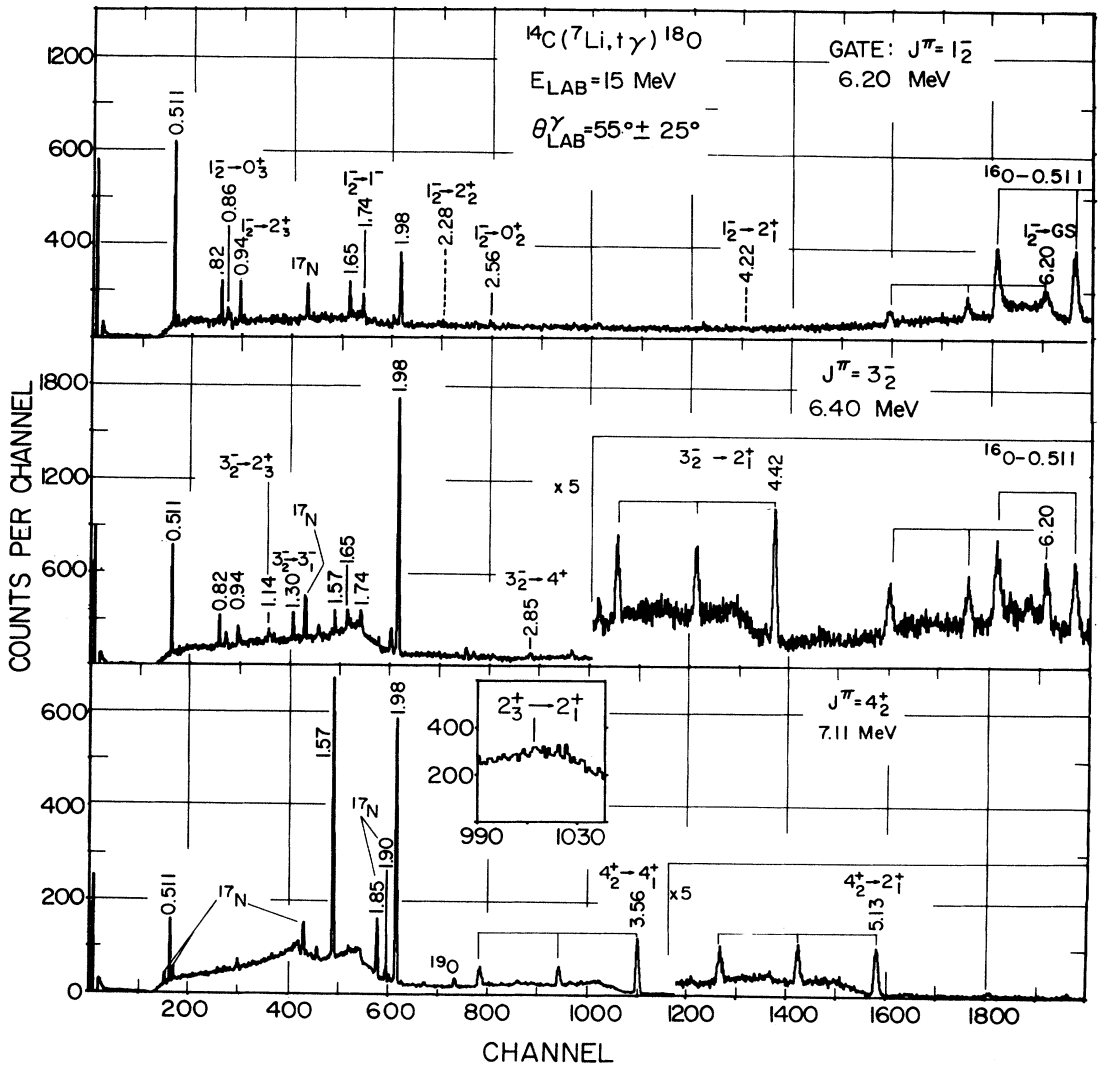

FIG. 4. Gamma-ray spectra in coincidence with specified triton groups. The expected location of the unobserved $1^-_2 \rightarrow 2^+_1$ and $1^-_2 \rightarrow 2^+_2$ transitions are indicated. Contaminant lines from ^{17}N and ^{19}O are identified. In the inset we show the energy region corresponding to the unobserved $2^+_3 \rightarrow 2^+_1$ transition, which would be associated with the unobserved $4^+_2 \rightarrow 2^+_3$ decay, as discussed in the text. The upper limit on this decay branching ratio extracted for this transition was confirmed more recently.[49]

deexcitations.

Collective states and band structure in ^{18}O. The ground state of ^{18}O and the $J^{\pi}=0^+_3$ state in ^{18}O have well understood two-neutron parentage. All the observed properties of the 0^+_3 state, including its Coulomb energy shift,[46] suggest that it is a member of the $|s^2_{1/2};T=1\rangle$ isospin triplet, which includes the corresponding states in ^{18}F and ^{18}Ne. The empirical wave functions of this state and of the 0^+ ground state[7] are very close to those based upon a simple quasispin model,[47,48] for example,

$$|0^+_{g.s.}\rangle \approx \sqrt{6/8}|d^2_{5/2}\rangle + \sqrt{2/8}|S^2_{1/2}\rangle ,$$
$$|0^+_3\rangle \approx \sqrt{2/8}|d^2_{5/2}\rangle - \sqrt{6/8}|S^2_{1/2}\rangle . \quad (2)$$

The identification of the $J^{\pi}=0^+_2$, 2^+_3, and 4^+_2 states in ^{18}O as collective states has been discussed at length in the literature (see, for example, Ref. 7), while other states are identified as simple two-neutron states expected within the framework of a simple $0\hbar\omega$ *sd* shell model. These collective positive-parity states are believed to have predominantly 4p-2h cluster structure and are suggested to form a collective quadrupole band. It appears that the $J^{\pi}=4^+_1$ state mixes with the collective state, as suggested by the weak $B(2^+_3 \rightarrow 4^+_1)=1.1(6)\%$ reported here, corresponding to an enhanced $B(E2\uparrow:4^+_1 \rightarrow 2^+_3)=11(6)$ W.u. In addition, the present upper limit of 0.6% on the $4^+_2 \rightarrow 2^+_3$ transition is confirmed in a recent experiment where it is measured[49] to be equal to $0.3^{\pm}0.08\%$, yielding a very small $B(E2:4^+_2 \rightarrow 2^+_3)=5.7$ (1.9) W.u. As discussed in Ref. 49 this small $B(E2)$ is in strong disagreement with

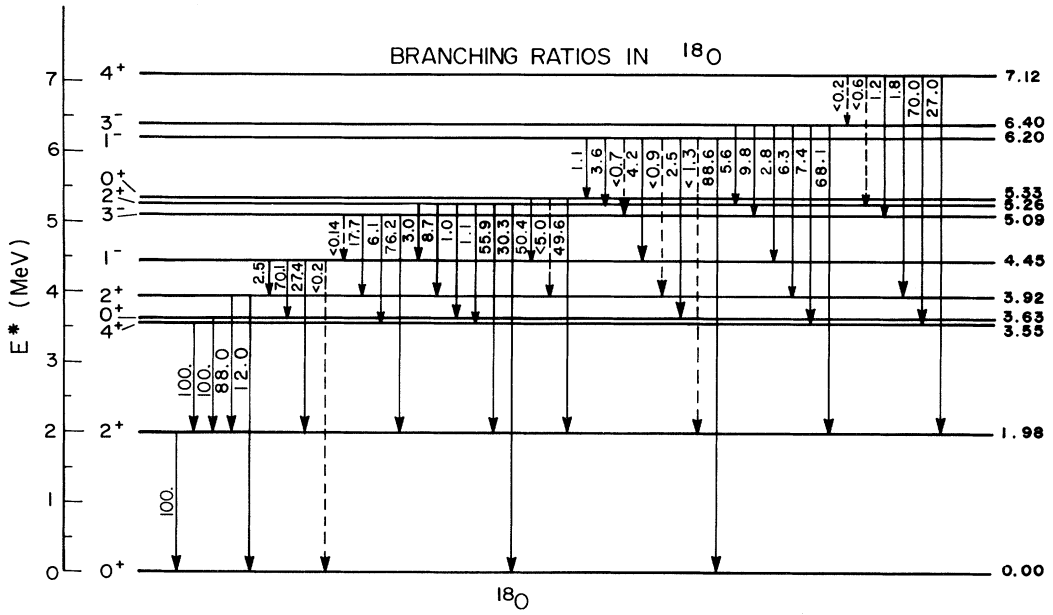

FIG. 5. Branching ratios for gamma-ray deexcitations in ^{18}O, as listed in Table I.

expectations based on a collective coexistence model identifying a collective band, including the $J^{\pi}=0_2^+$, 2_3^+, and 4_2^+ states.

Systematic data also indicate that the 1_1^- and 3_1^- negative-parity states are collective. The shell-model interpretation of these negative-parity states as $t+^{15}$N (Refs. 21 and 23) cluster states has an overlap with an $\alpha+^{14}$C parentage, used for the description of the positive-parity cluster states: consequently, both positive- and negative-parity states have *overlapping cluster structure.* We also note that the $J^{\pi}=3_3^-$ state in ^{18}O exhibits a large alpha particle width, $\theta_{\alpha}^2=24\%$,[45] again suggesting $\alpha+^{14}$C cluster parentage. Finally, we find a large alpha-particle spectroscopic factor[15–17] for the 1_2^- state, as large as that of the 1_1^- state, and small (t,p), two-neutron transfer cross section, smaller than that to the 1_1^- state. We thus conclude, based on the empirical data, that the 1_1^- and 1_2^- states are of similar structure, or substantially mixed. We now turn to the observed enhancement of $E1$ matrix elements linking these states in ^{18}O.

Selective enhanced E1's in ^{18}O. The most interesting result of our present study is the observation of selective enhanced $E1$ deexcitations. In Fig. 8 we show the deexcitation patterns of the four known 1^- states and two 3^-

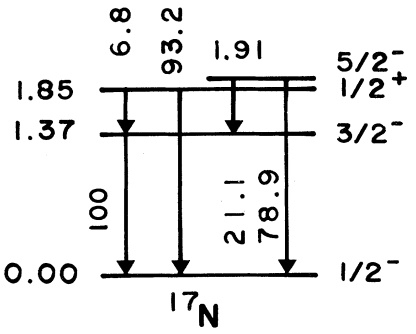

FIG. 6. Branching ratios for gamma-ray deexcitations in ^{17}N, as listed in Table II.

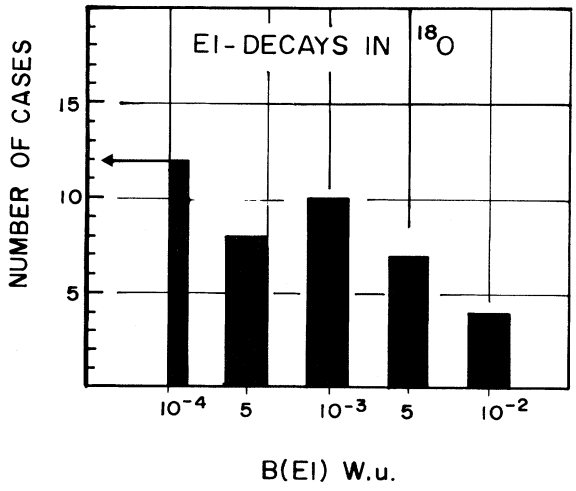

FIG. 7. Distribution of 41 measured $E1$ matrix elements in ^{18}O.

TABLE I. Branching ratios for gamma decays in ^{18}O.

E_i (MeV)	τ_i (psec)[a]	J_i^π	E_f (MeV)	J_f^π	Branching ratio (%) Present	Refs. 9, 12	Adopted[b]	$E\lambda$	$\lvert M(E\lambda)\rvert^2$ (W.u.)[c]
1.98	2.80(7)	2_1^+	0.00	0^+	100	100	100	$E2$	3.4(1)
3.55	24.8(12)	4_1^+	1.98	2^+	100	100	100	$E2$	1.2(1)
3.63	1.38(16)	0_2^+	1.98	2^+	100	100	100[e]	$E2$	↑3.4(4)
3.92	0.0238(25)[d]	2_2^+	0.00	0^+	11.1(10)	13.3(12)	12.0(11)	$E2$	1.5(2)
			1.98	2^+	88.9(10)	86.7(12)	88.0(11)	$M1$	0.16(2)
					$\delta=0.12(4)$			$E2$[f]	5.6(37)
4.45	0.065(15)	1_1^-	0.00	0^+	<0.2	<1	<0.2	$E1$	$<5.0\times10^{-7}$
			1.98	2^+	29.5(10)	25.0(11)	27.4(22)	$E1$	$\uparrow2.4(6)\times10^{-4}$
			3.63	0_2^+	68.9(10)	71.6(11)	70.1(13)	$E1$	$2.8(7)\times10^{-2}$
			3.92	2_2^+	1.6(2)	3.4(2)	2.5(9)	$E1$	$\uparrow2.2(10)\times10^{-3}$
5.10	0.062(25)	3_1^-	1.98	2^+	76.5(10)	75.0(20)	76.2(9)	$E1$	$5.7(23)\times10^{-4}$
			3.55	4^+	5.6(10)	8.0(20)	6.1(10)	$E1$	$\uparrow2.9(13)\times10^{-4}$
			3.92	2_2^+	17.9(8)	17.0(20)	17.7(8)	$E1$	$2.5(10)\times10^{-3}$
			4.45	1^-	<0.14		<0.14	$E2$	<57
5.26	0.0110(7)[g]	2_3^+	0.00	0^+	30.3(9)	32.0(30)	30.3(9)	$E2$	2.0(1)[g]
			1.98	2^+	55.9(10)	68.0(30)	55.9(10)	$M1$	$4.5(3)\times10^{-2}$
					$\delta=0.15(4)$			$E2$[f]	0.9(5)
			3.55	4^+	1.1(6)		1.1(6)	$E2$	↑11.3(60)
			3.63	0_2^+	1.0(6)		1.0(6)	$E2$	23.0(14)
			3.92	2_2^+	8.7(4)		8.7(4)	$M1$[h]	0.10(8)
			4.45	1^-	3.0(3)		3.0(3)	$E1$	$7.4(9)\times10^{-3}$
5.34	0.20(4)	0_3^+	1.98	2^+	45.2(50)	54.0(50)	49.6(44)	$E2$	↑0.3(1)
			3.92	2_2^+	<12.0	<5.0	<5.0	$E2$	↑<3.0
			4.45	1^-	54.8(50)	46.0(50)	50.4(44)	$E1$	$\uparrow1.7(4)\times10^{-3}$
6.20	0.0033(6)[i]	1_2^-	0.00	0^+	88.7(9)	88.0(20)	88.6(9)	$E1$	$1.6(3)\times10^{-3}$
			1.98	2^+	<1.3		<1.3	$E1$	$<5.6\times10^{-5}$
			3.63	0_2^+	2.5(3)		2.5(3)	$E1$	$6.4(13)\times10^{-4}$
			3.92	2_2^+	<0.9		<0.9	$E1$	$<2.5\times10^{-4}$
			4.45	1^-	4.1(4)	6.0(20)	4.2(4)	$M1$[h]	$7.5(15)\times10^{-2}$
			5.09	3^-	<0.7		<0.7	$E2$	↑<71
			5.26	2_3^+	3.6(4)		3.6(4)	$E1$	$\uparrow1.1(2)\times10^{-2}$
						6.0(30)			
			5.34	0_3^+	1.1(3)		1.1(3)	$E1$	$7.4(24)\times10^{-3}$

TABLE I. (*Continued*).

E_i (MeV)	τ_i (psec)[a]	J_i^π	E_f (MeV)	J_f^π	Branching ratio (%) Present	Refs. 9, 12	Adopted[b]	$E\lambda$	$\lvert M(E\lambda)\rvert^2$ (W.u.)[c]
6.40	0.030(15)	3_2^-	1.98	2^+	68.1(18)	90.0(50)	68.1(18)	$E1$	$3.7(19)\times10^{-4}$
			3.55	4^+	7.4(12)		7.4(12)	$E1$	$\uparrow 1.2(6)\times10^{-4}$
			3.92	2_2^+	6.3(10)	10.0(50)	6.3(10)	$E1$	$1.9(10)\times10^{-4}$
			4.45	1^-	2.8(10)		2.8(10)	$E2$	9.7(60)
			5.09	3^-	9.8(9)		9.8(9)	$M1$[h]	$4.6(23)\times10^{-2}$
			5.26	2_3^+	5.6(9)		5.6(9)	$E1$	$1.8(9)\times10^{-3}$
7.12	0.0025(7)[i]	4_2^+	1.98	2^+	27.0(5)	40.0(100)	27.0(5)	$E2$	3.3(8)
			3.55	4^+	70.0(10)	60.0(100)	70.0(10)	$M1$	$7.3(33)\times10^{-2}$
	$\Gamma_\gamma/\Gamma=0.48(10)$				<0.3		<0.3	$E2$[f]	<0.15
			3.92	2_2^+	1.8(4)		1.8(4)	$E2$	2.3(6)
			5.09	3^-	1.2(3)		1.2(3)	$E1$	$3.1(8)\times10^{-4}$
			5.26	2_3^+	<0.6		<0.6	$E2$	<12
			6.40	3_2^-	<0.2		<0.2	$E1$	$<1.2\times10^{-3}$

[a]Lifetime data from Ref. 1 unless otherwise specified.
[b]Average weighted by error bars was used.
[c]$B(E\lambda)$'s are listed from high to low spin, in all cases.
[d]From the (e,e') result of Ref. 19: $B(E2{:}0^+\rightarrow2^+)=22.2(10)\ e^2\text{fm}^4$ and the adopted branching ratios, we obtain $\tau=23.\dot{8}(25)$ fsec; in excellent agreement with the less accurate direct lifetime measurement of Ref. 9: $\tau=24(10)$ fsec.
[e]$0^+\rightarrow0^+B$ of 0.030(6)% is reported.[1].
[f]Mixing ratios (δ) quoted are from Ref. 9.
[g]From (e,e') data of Ref. 19, deduced lifetime is based on the adopted branching ratios reported here.
[h]Assumed $\delta=0$.
[i]From (γ,γ') data of Ref. 11, deduced lifetime is based on the adopted branching ratios reported here.
[j]From $\Gamma_\alpha/\Gamma_\gamma=0.9(1)$ of Ref. 1 and $\Gamma_\gamma=0.095(20)$ eV of Ref. 45, we deduce $\Gamma=0.26(6)$ eV.

TABLE II. Branching ratios for gamma decays in ^{17}N.

E_i	J_i^π	E_f	J_f^π	Branching ratio (%) [a]	[b]	Present	Adopted[c]
1.85	$\frac{1}{2}^+$	0.0	$\frac{1}{2}^-$	83(3)	90(3)	94.7(10)	93.2(25)
		1.374	$\frac{3}{2}^-$	17(3)	10(3)	5.3(10)	6.8(25)
1.91	$\frac{5}{2}^-$	0.0	$\frac{1}{2}^-$	74(4)	78(3)	82.5(30)	78.9(23)
		1.374	$\frac{3}{2}^-$	26(4)	22(3)	17.5(30)	21.1(23)

[a]Guillaume *et al.*, Nucl. Phys. **A272**, 338 (1976).
[b]D.W.O. Rogers *et al.*, Nucl. Phys. **A226**, 424 (1974); **A226**, 445 (1974).
[c]Average weighted by error bars was used.

states in ^{18}O. Some of these data are taken from our previously reported work[45] on radiative capture of alpha particles by ^{14}C.

We first examine the deexcitation of the 3_3^- state,[45] for which the selective $E1$ matrix elements are most clearly evident. The $J^\pi=3_3^-$ state (which is known to have large alpha cluster parentage, $\theta_\alpha^2=24\%$) deexcites preferentially to the collective 2_3^+ state, and the transitions to the lower-lying two-neutron 2^+ states (which should be favored as a consequence of the larger transition energy) are not observed. The upper limits established for the corresponding branching ratios would indicate $B(E1)$ reduced matrix elements which are some 2 orders of magnitude smaller than the observed enhanced $B(E1\colon 3_3^-\rightarrow 2_3^+)=1.4(3)\times10^{-2}$ W.u. For the two-neutron states we find hindrance of $B(E1)$'s of the magnitude usually found in even-even nuclei. We note in Fig. 8 that the $J^\pi=3_3^-$ state exhibits a mildly enhanced $E1$ deexcitation, with $B(E1\uparrow:4^+\rightarrow 3^-)=4.7(12)\times10^{-3}$ W.u. However, as noted above, this 4_1^+ state acquires an

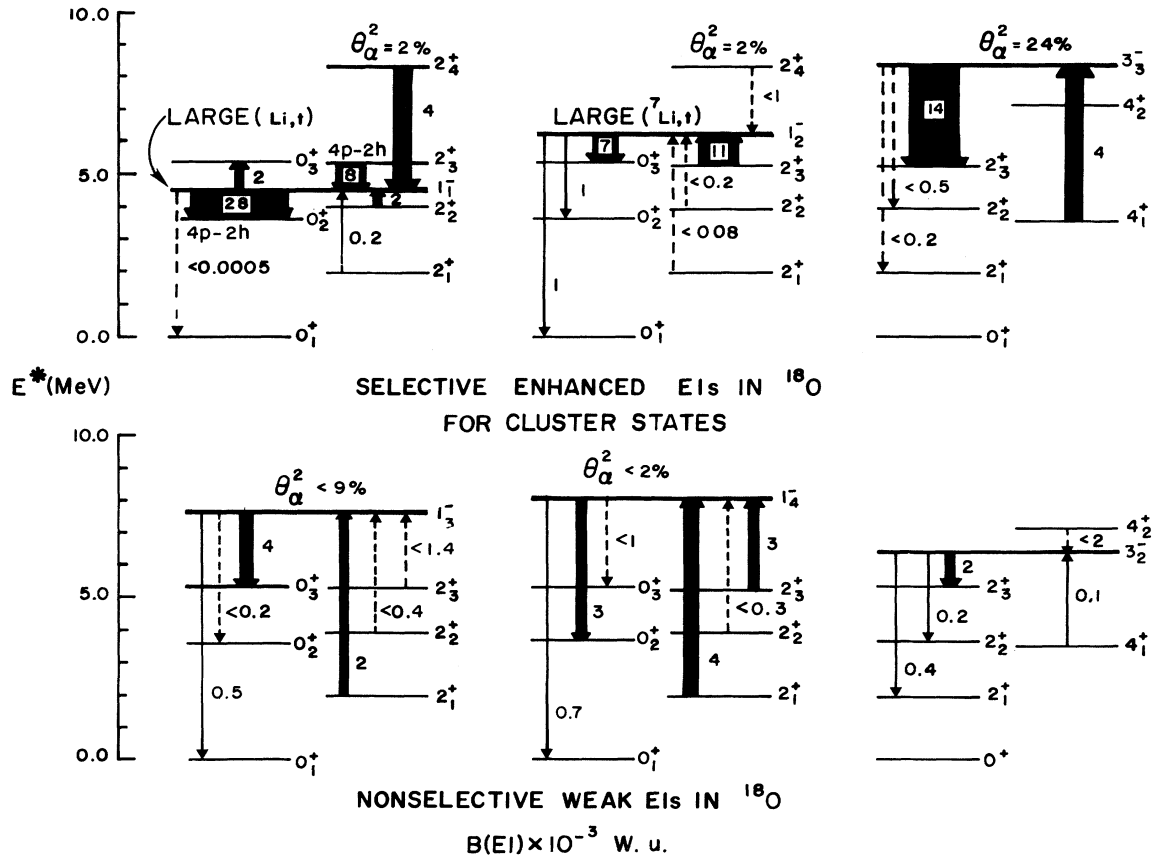

FIG. 8. Characteristics of enhanced $E1$ transitions in ^{18}O. All enhanced $E1$ transitions measured in ^{18}O are shown, exhibiting a correlation with cluster structure as discussed in the text.

admixture from the collective 4^+ state and the observed weak enhancement of the $B(E1)$ reduced matrix element may reflect that collective admixture.

In contrast, the noncollective $J^\pi = 3_2^-$ state displays all possible $E1$ deexcitation modes with no apparent selectivity, as shown in Fig. 8. However, the strongest observed $B(E1)$ from this state is again that to the collective 2_3^+ state, and all other $B(E1)$ values are between 10^{-3} and 10^{-4} W.u., as characteristic of $B(E1)$ transitions in light even-even nuclei. The 3_2^- state is not considered to be a collective state, and it exhibits nonselective weak $E1$ deexcitations. The 1_3^- and 1_4^- states also have small alpha particle reduced widths and, as shown in Fig. 8, these states again exhibit nonselective weak $E1$ decays.

The deexcitation of the collective 1_1^- state, shown in Fig. 8, is also very selective. In this case the enhanced $E1$ deexcitation is preferentially to the well known 4p-2h 0_2^+ state and not to any of the other lower-lying 0^+ states; in Fig. 3 we indicate in the observed spectrum where the transition to the two-neutron $d_{5/2}^2(0^+)$ ground state would have been expected. A less clear situation exists for the matrix elements connecting this 1_1^- state to 2^+ states. While we observe an enhanced $E1$ to the collective 2_3^+ state, we also find a somewhat smaller, but still enhanced $B(E1)$ to the 2_4^+ state (see Fig. 8). Again the situation here suggests a mixing of the 2_3^+ and 2_4^+ states, as discussed earlier in this paper and in Ref. 29. A recent study of $^{18}O(e,e')^{18}O^*$ by Manley *et al.*[50] suggests a considerable mixing of 4p-2h amplitude in the 2_4^+ state at 8.29 MeV. This result may justify remeasuring the alpha-particle width of the 2_4^+ state, quoted as $\Gamma(\text{lab}) = 1.6 \pm 1.0$ keV, with $\theta_\alpha^2 = 2.0 \pm 1.5\,\%$, as shown in Fig. 8.

The $J^\pi = 1_2^-$ state also deexcites preferentially by an enhanced $E1$ transition to the collective 2_3^+ state, but not to any of the other lower-lying 2^+ states in ^{18}O. In Fig. 4 we indicate, in the measured spectrum, the expected location of the unobserved transitions. Again, the enhanced $B(E1)$ to the collective 2_3^+ state, and the absence of any transition to two-neutron low-lying 2^+ states, suggests that the $B(E1)$ enhancement reflects cluster parentage of the states involved.

A correlation of enhanced E1 deexcitations [$B(E1) > 2.0 \times 10^{-3}$ W.u.] and alpha-particle spectroscopic factors. A hint to the origin of the enhanced $E1$'s can be found by considering alpha-particle spectroscopic factors of the states involved in the enhanced $E1$ decay. Here we only consider $B(E1) > 2.0 \times 10^{-3}$ W.u., larger than the measured mean (see above) of $B(E1) = 1.6 \times 10^{-3}$ W.u. Weak $B(E1)$'s ($< 10^{-3}$ W.u.) may arise for a number of reasons such as cancellations, complicated structure, etc. Consequently, in general, weak $E1$'s do not reveal nuclear-structure information, and therefore are not considered here. In Fig. 9 we plot enhanced $E1$ transitions in ^{18}O measured in this work against the experimentally measured[17] alpha-particle spectroscopic factors for the initial and final states involved in the deexcitations.

Unfortunately, for a few states measured in the radiative capture work[45] alpha-particle spectroscopic factor information is not available, and hence these states cannot be included here. However, we emphasize that for these higher-lying states the alpha-particle reduced widths are measured, as plotted in Fig. 8, and in this case nonselective weak $B(E1)$'s are shown to be found for the noncluster states, characterized by small alpha-particle reduced widths ($\theta_\alpha^2 \approx$ a few percent). The $B(E1)$'s are converted for all transitions to have the initial state of higher spin. The alpha-particle spectroscopic factors were extracted from (^{6}Li,d) data and are listed separately[17] for negative-(S_7) and positive-(S_8) parity states, and we therefore use in our plot an arbitrary unit for the spectroscopic factors.

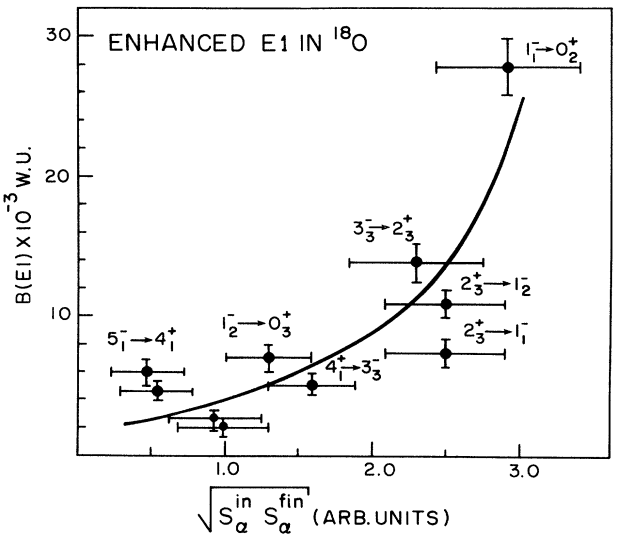

FIG. 9. Enhanced $E1$ deexcitations [$B(E1) > 2.0 \times 10^{-3}$ W.u.] plotted against alpha-particle spectroscopic factors of the initial and final states. All known spectroscopic factors are plotted as deduced from (^{6}Li,d) data and given in Ref. 17. A clear correlation of $E1$ enhancement and large alpha-particle spectroscopic factors is observed with deviation only for the $B(E1{:}2_3^+ \rightarrow 1^-) = 7.5(7) \times 10^{-3}$ W.u., as discussed in text.

We clearly observe a correlation of the $B(E1)$ values of enhanced $E1$ deexcitations [$B(E1) > 2.0 \times 10^{-3}$ W.u.] and alpha-particle spectroscopic factors, with one data point, the $B(E2{:}2_3^+ \rightarrow 1_1^-) = 7.5(7) \times 10^{-3}$ W.u., deviating significantly from the smooth line drawn in the figure. However it appears that the data are consistent with a mixing of the two 2_3^+ and 2_4^+ states, which leads to a spreading of the $E1$ strength. In fact, it appears that the data on enhanced $B(E1)$'s suggest an almost linear dependence of $B(E1)$ values on $S_\alpha^{\text{initial}} S_\alpha^{\text{final}}$, as would be expected if the enhanced $B(E1)$'s arose from cluster structures. We emphasize again that this correlation is based only on experimental data.

While we have demonstrated that enhanced $E1$'s arise from states of large alpha-particle spectroscopic factors, the contrary is not claimed. Namely, states with large alpha-particle spectroscopic factors do not necessarily ex-

hibit enhanced $E1$'s. In Ref. 31 it is suggested that only a subset of alpha-cluster states, denoted as cluster-molecular states, exhibit enhanced $E1$'s. In a cluster-molecular state the alpha-particle is well separated from the $A-4$ core nucleus.

We then conclude, based on the data shown in Fig. 8, and the correlation shown in Fig. 9, that there exists a correlation between enhanced $E1$ deexcitations and cluster states in ^{18}O. We further suggest the following as *empirical deexcitation* general guide lines for $E1$ enhancement in ^{18}O:

(a) In the case that both initial and final states are cluster states (i.e., either $\alpha+^{14}C$ or $t+^{15}N$ cluster states) the enhanced $E1$'s are at the level of $\geq 10^{-2}$ W.u.

(b) In the case that one of the states is of cluster nature and the second is considerably admixed, the $B(E1)$'s are at the level of $(3\text{–}6)\times 10^{-3}$ W.u.

(c) In the case that both initial and final states are simple two-neutron states the $B(E1)$'s are hindered at the level of $\leq 10^{-3}$–10^{-4} W.u.

Corresponding behavior is evident for collective enhanced $E2$ deexcitations as observed for example in ^{20}Ne. Such correlations between enhanced $E1$ deexcitations and collective states is established here for the first time as an empirical correlation, suggesting a collective origin for enhanced $E1$'s in ^{18}O.

Application of a vibron model to ^{18}O. We have carried out a preliminary application of the vibron model[24,25] to our data in the limiting symmetries [O(4) and U(3)] of this U(4) model. We present here the model calculations as a way of introducing this vibron model, without drawing any firm conclusion with respect to the interpretation of the data.

All predictions of energy and deexcitation matrix elements in these cases are given in closed-form analytic expressions.[51] In the U(3) limit[24,25] the energy spectrum is given by

$$E(n,L)=\epsilon n+BL(L+1) \tag{3}$$

with n counting the number of dipole phonons and ϵ its energy. We assumed B to be small, corresponding to harmonic oscillations in three dimensions. The matrix elements of the dipole operator are then related to the number of dipole phonons n, total number of bosons N, and the angular momentum of the state. For example, for a stretched intraband $E1$ decay we find[51]

$$\langle [N],n,L\|(s\tilde{p})^{(1)}\|[N],n-1,L-1\rangle = \sqrt{L(n+L+1)(N-n+1)}\ . \tag{4}$$

In the O(4) limit, on the other hand, the energy spectrum is given by

$$E(v,L)=Av(N-v+1)+BL(L+1) \tag{5}$$

with v labeling the vibrational bandhead in this vibration-rotation picture, and given by $v=(N-\sigma)/2$ with $\sigma=N,\ N-2,\ \ldots,\ 0$ or 1. The constant B

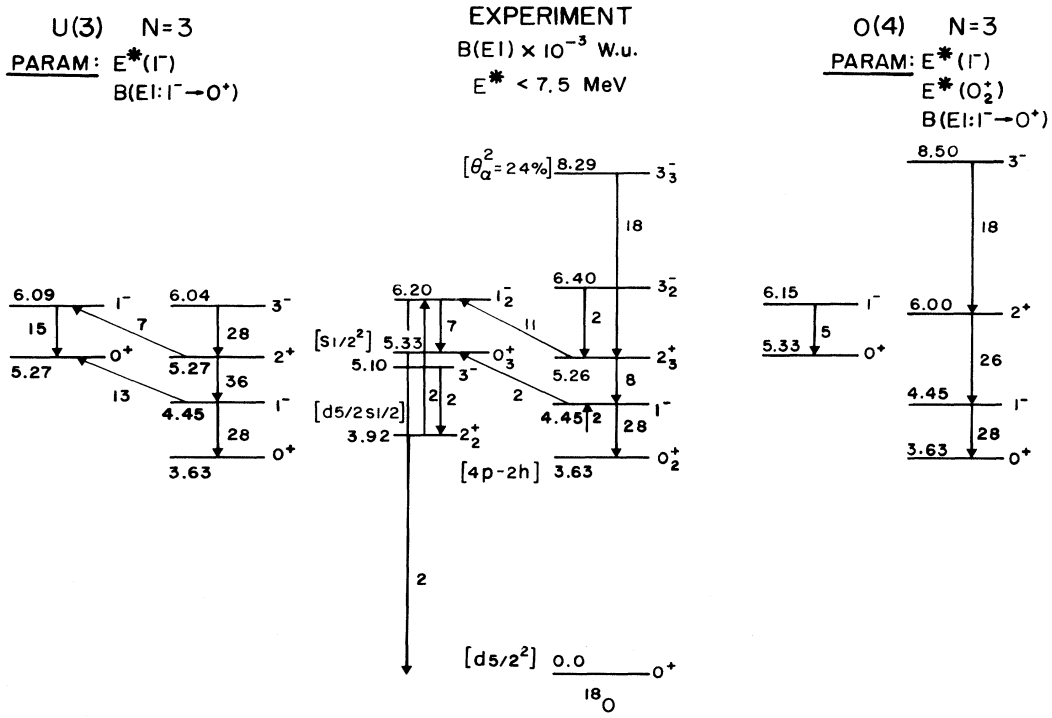

FIG. 10. Comparison between the predictions of the vibron model[24,25,50] in its two limiting symmetries, and the data reported herein. All $E1$ transitions from states below 7.5 MeV and having reduced matrix elements larger than 2×10^{-3} W.u. are shown. As discussed in the text, existing data suggest that the 0_3^+ state is of two-neutron $(s_{1/2})^2$ character and therefore is not included in the collective vibron model space.

represents the moment of inertia of the dipole band, $B=\hbar^2/2I=0.35$ MeV, as compared to the classical moment of inertia of two touching $\alpha+^{14}C$ spheres, with $B=0.29$ MeV for $R_0=1.2$ fm. In this O(4) limit only intraband decays are allowed with

$$\langle [N],\sigma,L+1\|(ps+s\tilde{p})^{(1)}\|[N],s,L\rangle = \sqrt{(\sigma-L)(\sigma+L+2)(L+1)} . \quad (6)$$

We have calculated the spectra predicted in these two limits and the matrix elements of the $E1$ operator using equations 3 through 6. In the U(3) limit there is only a single free parameter associated with the matrix elements and one with the energy of states (the dipole phonon energy); in the O(4) limit, two parameters are needed to reproduce the state energies. The model parameters are shown in Fig. 10. The effective number of bosons is a free parameter, but the exact value of the $B(E1)$ reduced matrix element is not sensitive to it, and its major effect is on the number of states predicted by the model.

The predictions of a vibron model for $E1$ transitions in ^{18}O are compared to our data in Fig. 10. All $E1$'s are predicted to within factors of 3–4, despite the small number of free parameters and the fact that we have assumed limiting symmetries. However, in this description the 0_3^+ is assumed to be collective, contrary to our previous discussion, see Eq. (2). If we assume an O(4) limit, $E1$ transitions between different bands (interband) are forbidden, and the observed interband transitions may arise from mixing between states in different bands and from breaking of the O(4) symmetry. It should be emphasized that transition amplitudes involving two-neutron states are not included in this model space. If we assume a U(3) symmetry, interband $E1$ transitions are allowed but the transition between the excited 1_2^- and the first 0^+ states, for example, are forbidden, since they correspond to two dipole phonon transitions.

V. CONCLUSIONS

We report herein a detailed study of the deexcitation of all the natural parity states in ^{18}O up to the alpha-particle threshold; these data are complementary to those reported earlier from a study of the radiative capture of alpha particles by ^{14}C. A strong empirical correlation between enhanced $E1$ and cluster states is established, based on observation of the strong selectivity of these $E1$ deexcitation. This *empirical correlation* established here for $E1$ transitions for the first time, suggests a collective origin for $E1$ enhancements in ^{18}O. We attempt to fit the data with a vibron model at its limiting symmetries, and point out both the successes and failures of the model.

This work was supported by U. S. Department of Energy Contract No. DE-AC02-76ER03074.

*Current address: Schlumberger, Montrouge, CEDEX, France.
†Current address: The White House, Washington, D.C. 20500.

[1]F. Ajzenberg-Selove, Nucl. Phys. **A475**, 1 (1987).
[2]H. Morinaga, Phys. Rev. **92**, 254 (1956).
[3]G. E. Brown and A. M Green, Nucl. Phys. **85**, 87 (1966).
[4]P. Federman and I. Talmi, Phys. Lett. **19**, 490 (1965).
[5]L. Zamick, Phys. Lett. **1**, 580 (1965).
[6]A. Arima, H. Horiuchi, and T. Sebe, Phys. Lett. **24B**, 129 (1967).
[7]R. D. Lawson, F. J. D. Serduke, and H. T. Fortune, Phys. Rev. C **14**, 1245 (1976).
[8]R. Moreh, Nucl. Phys. **A97**, 106 (1967).
[9]J. W. Olness, E. K. Warburton, and J. A. Becker, Phys. Rev. C **7**, 2239 (1973).
[10]J. A. Becker, L. F. Chase, Jr., D. Kohler, and R. E. McDonald, Phys. Rev. C **8**, 2007 (1973).
[11]M. Hass, Z. Shkedi, D. F. H. Start, Y. Wolfson, and Y. S. Horowitz, Nucl. Phys. **A220**, 217 (1974).
[12]J. W. Olness, E. K. Warburton, D. E. Alburger, C. J. Lister, and D. J. Millener, Nucl. Phys. **A373**, 13 (1982).
[13]M. E. Cobern, L. C. Bland, H. T. Fortune, G. E. Moore, S. Mordechai, and R. Middleton, Phys. Rev. C **23**, 2387 (1981).
[14]S. Hinds, H. Marchant, and R. Middleton, Nucl. Phys. **38**, 81 (1962).
[15]G. L. Morgan, D. R. Tilley, G. E. Mitchell, R. A. Hilko, and N. R. Roberson, Phys. Lett. **32B**, 353 (1970).
[16]L. M. Martz, S. J. Sanders, and P. D. Parker, *Contributed Papers to the International Conference on Nuclear Structure, Tokyo, 1977,* edited by T. Marumori (Physical Society of Japan, Tokyo, 1978) p. 177.
[17]A. Cunsolo, A. Fotti, G. Imme, G. Pappalardo, and G. Raciti, Phys. Rev. C **24**, 476 (1981).
[18]J. Janecke and F. D. Becchetti, Proceedings of the Nuclear Physics Workshop, Trieste, Italy, 1981 (unpublished).
[19]B. E. Norum, M. V. Hynes, H. Miska, W. Bertozzi, J. Kelly, S. Kowalski, F. N. Rad, C. P. Sargent, T. Sasanuma, W. Turchinetz, and B. L. Berman, Phys. Rev. C **25**, 1778 (1982).
[20]H. T. Fortune and S. C. Headley, Phys. Lett. **51B**, 136 (1974).
[21]D. J. Millener and D. Kurath, Nucl. Phys. **A255**, 315 (1975); and D. J. Millener, private communication, 1982.
[22]T.-S.H. Lee and R. D. Lawson, Phys. Rev. C **21**, 679 (1980).
[23]B. Buck and A. A. Pilt, Nucl. Phys. **A295**, 1 (1978).
[24]F. Iachello, Phys. Rev. C **23**, 2778 (1981); and Nucl. Phys. **A396**, 233c (1983).
[25]F. Iachello and A. D. Jackson, Phys. Lett. **108B**, 151 (1982).
[26]B. Buck and A. A. Pilt, Nucl. Phys. **A280**, 133 (1977).
[27]L. A. Radicati, Phys. Rev. **87**, 521 (1952).
[28]M. Gell-Mann and V. T. Telegdi, Phys. Rev. **91**, 169 (1953).
[29]M. Gai, M. Ruscev, A. C. Hayes, J. F. Ennis, R. Keddy, E. C. Schloemer, S. M. Sterbenz, and D. A. Bromley, Phys. Rev. Lett. **50**, 239 (1983).
[30]M. Ruscev, Ph.D. thesis, Yale University, 1983 (unpublished).
[31]Y. Alhassid, M. Gai, and G. F. Bertsch, Phys. Rev. Lett. **49**, 1482 (1982).
[32]M. R. Strayer, R. Y. Cusson, A. S. Umar, P.-G. Reinhard, D. A. Bromley, and W. Greiner, Phys. Lett. **135B**, 261 (1984).
[33]H. J. Assenbaum, K. Langanke, and A. Weiguny, Z. Phys. **A318**, 35 (1984).

[34]W. Wintgen, H. Friedrich, and K. Langanke, Nucl. Phys. **A408**, 239 (1983).
[35]P. Descouvemont and D. Baye, Phys. Rev. C **31**, 2274 (1985).
[36]Y. Suzuki, A. Yamamoto, and K. Ikeda, Nucl. Phys. **A444**, 365 (1985).
[37]B. A. Brown, private communication, 1982.
[38]A. C. Hayes, D. J. Millener, and D. A. Bromley (unpublished).
[39]We thank J. L. Gallant of the Chalk River Nuclear Laboratories, Canada, for providing the ^{14}C targets.
[40]Yamazaki, Nucl. Data **A3**, 1 (1967).
[41]E. Der Mateosian and A. W. Sunyar, At. Data Nucl. Data Tables **13**, 391 (1974).
[42]W. D. Hamilton, in *The Electromagnetic Interaction in Nuclear Spectroscopy,* edited by W. D. Hamilton (North-Holland, Amsterdam, 1975), p. 645.
[43]G. J. McCallum and G. E. Coote, Nucl. Instrum. Methods **124**, 309 (1975).
[44]R. A. Meyer and T. N. Massey, ICRM Seminar on Applied Radionuclide Metrology, Geel, Belgium, 1983 (unpublished); Lawrence Livermore Laboratory Report No. UCRL-89142.
[45]M. Gai, R. Keddy, D. A. Bromley, J. W. Olness, and E. K. Warburton, Phys. Rev. C **36**, 1256 (1987).
[46]A. V. Nero, E. G. Adelberger, F. S. Dietrich, and G. E. Walker, Phys. Rev. Lett. **32**, 623 (1974).
[47]A. K. Kerman, Ann. Phys. **12**, 300 (1961).
[48]M. Gai, A. Arima, and D. Strottman, Phys. Lett. **106B**, 6 (1981).
[49]M. Gai, S. L. Rugari, R. H. France III, B. J. Lund, Z. Zhao, D. A. Bromley, B. A. Lincoln, W. W. Smith, M. J. Zarcone, and Q. C. Kessel, Phys. Rev. Lett. **62**, 874 (1989).
[50]D. M. Manley, D. J. Millener, B. L. Berman, W. Bertozzi, T. N. Buti, J. M. Finn, F. W. Hersman, C. E. Hyde-Wright, M. V. Hynes, J. J. Kelly, M. A. Kovash, S. Kowalski, R. W. Lourie, B. Murdock, B. E. Norum, B. Pugh, and C. P. Sargent, Phys. Rev. C **41**, 448 (1980).
[51]O. van Roosmalen, Ph.D. thesis, KVI-Groningen, 1980 (unpublished).